Excitation Functions for (α,xn) Reactions on Lead*

WALTER JOHN, JR.†
Radiation Laboratory, Physics Department, University of California, Berkeley, California
(Received March 20, 1956)

The excitation functions for alpha-induced reactions on lead have been measured. A procedure has been developed for preparing enriched lead isotope targets by evaporation. Stacked foils were bombarded by the alpha-beam of the 60-inch cyclotron. The induced polonium alpha activities were separated by alpha pulse-height analysis.

The measured excitation functions for $Pb^{206}+\alpha$ are compared to the excitation functions for $Bi+p$. Since the compound nucleus formed is the same, the comparison gives a test of the predictions of Bohr's compound nucleus theory. The ratios of corresponding cross sections are in agreement with the compound nucleus theory. However, the excitation functions are displaced in energy by an amount not predicted by the theory. The disagreement is just outside of the experimental errors. The comparison of $Ni^{60}+\alpha$ and $Cu^{63}+p$ made by Ghoshal has been checked with more recent mass values, revealing a larger energy discrepancy.

The excitation functions for reactions on various lead isotopes are found to be very similar. However, the excitation functions are found to be displaced in energy by an amount not exactly equal to the differences in thresholds.

I. INTRODUCTION

ACCORDING to the compound-nucleus theory of Bohr,[1] a nuclear reaction proceeds in two stages: firstly the formation of a compound system and secondly the breakup of this compound system. The breakup and formation are independent processes. This concept can be justified in the region of isolated resonances. However, for the excitation energies obtaining in the medium-energy region, there is a large overlapping of levels and the compound-nucleus assumption cannot be rigorously made. Nevertheless, in order to make practical calculations for reactions, the compound-nucleus assumption is extended to the region of overlapping levels. In this region the justification for Bohr's assumption rests on comparison to experiment.

Ghoshal[2] tested the applicability of Bohr's assumption to the medium-energy region. According to Bohr we may write a reaction

$$\sigma(a,b)=\sigma_c(a)G_c(b),$$

where $\sigma_c(a)$ is the cross section for formation of the compound nucleus C with the incident particle a and $G_c(b)$ is the probability of breakup of the compound nucleus with the emission of products b. $G_c(b)$ depends only on the excitation energy of C and not on the method of formation. We may then derive the following relation:

$$\frac{\sigma(a,b)}{\sigma(a,b')}=\frac{G_c(b)}{G_c(b')}=\frac{\sigma(a',b)}{\sigma(a',b')}.$$

Ghoshal bombarded Ni^{60} with 40-Mev α particles and Cu^{63} with 32-Mev protons. In both cases the resulting compound nucleus is Zn^{64}. The relation

$$\sigma(p,n):\sigma(p,2n):\sigma(p,pn)=\sigma(\alpha,n):\sigma(\alpha,2n):\sigma(\alpha,pn)$$

was observed to hold when 7 Mev was added to the proton energy to match the excitation energy of the compound nucleus. The prediction of Bohr's assumption was thus verified.

The present experiment was undertaken in order to extend the test of Bohr's assumption to the region of the heavy elements. The excitation functions measured here for the $Pb^{206}(\alpha,xn)$ reactions are compared to the excitation functions for the $Bi^{209}(p,xn)$ reactions measured by Kelly.[3]

II. ALPHA-INDUCED REACTIONS ON LEAD

Alpha-induced reactions on lead were studied by Templeton, Howland, and Perlman.[4] The Po products were studied but excitation functions were not made. Spiess[5] has measured excitation functions for $Pb^{208}(\alpha,n)$ and $Pb^{208}(\alpha,p)$.

In this experiment the excitation functions for (α,xn) reactions on lead were measured by bombarding stacked foils in the 48-Mev alpha beam of the 60-inch cyclotron. The induced Po alpha activities were identified and separated by pulse-height analysis, since some of the half-lives are too long for decay analysis within a reasonable time. The reactions on the various lead isotopes were separated by the use of separated lead isotope targets.

The reactions on Pb^{204} were practically absent in the enriched isotope targets due to the very low abundance of Pb^{204}. The (α,γ) reactions are expected to give negligible interference owing to the small cross section. The maximum observed cross section for $Bi^{209}(p,\gamma)$ was less than 1 mb.[3] The maximum cross sections of the (α,xn) reactions are of the order of 1 barn. Only two reactions leading to alpha emitters involve proton emission. These are $Pb^{207}(\alpha,p)Bi^{210}$ and $Pb^{208}(\alpha,pn)Bi^{210}$. Bi^{210} beta-decays into Po^{210}, an alpha emitter. The cross sections for these reactions were not measured in this

* This work was supported by the U. S. Atomic Energy Commission.
† Present address: Department of Physics, University of Illinois, Urbana, Illinois.
[1] N. Bohr, Nature **137**, 344 (1936).
[2] S. N. Ghoshal, Phys. Rev. **80**, 939 (1950).
[3] E. L. Kelly, University of California Radiation Laboratory Report UCRL-1044, December 1950 (unpublished).
[4] Templeton, Howland, and Perlman, Phys. Rev. **72**, 758 and 766 (1947).
[5] F. N. Spiess, Phys. Rev. **94**, 1292 (1954).

experiment; however, they are expected to give little interference. Spiess[5] found the cross section for $Pb^{208}(\alpha,p)Bi^{211}$ to increase with increasing energy to 4 mb at the maximum energy of 39 Mev. Hence the $Pb^{207}(\alpha,p)Bi^{210}$ reaction is not expected to give appreciable interference here. Spiess also observed the excitation function for $Bi^{209}(\alpha,pn)Po^{211}$ (25-sec state only). The cross section increased with energy to 1 mb at 39 Mev. Templeton, Howland, and Perlman[4] found the cross section for $Pb^{208}(\alpha,pn)Bi^{210}$ to be 8 mb$\pm\sim$20% at 40 Mev. It is therefore concluded that the reaction $Pb^{208}(\alpha,pn)Bi^{210}$ does not interfere below 40 Mev. From 40 to 50 Mev, however, it may increase to an appreciable fraction of the Po^{210} high-energy tail here attributed to $Pb^{208}(\alpha,2n)Po^{210}$. All higher-order reactions have been neglected, since the cross sections are expected to be even smaller than those considered above. None of them leads to alpha emitters. Since their cross sections are small they do not appreciably affect the (α,xn) reactions through competition.

III. EXPERIMENTAL METHODS

A. Preparation of Targets

The targets were made by evaporation of lead in vacuum onto 0.0005-inch 2*SH* aluminum foil backing. Foil blanks approximately $\frac{1}{2}$ by $\frac{3}{4}$ inch were stamped by a die. The bombarded portion was approximately $\frac{1}{8}$ by $\frac{1}{2}$ inch. The thickness of the lead deposit was about 1 mg/cm^2. It was measured to better than 1% by weighing on an assay balance. This thickness provided reasonable counting rates, kept self-absorption corrections small, and introduced negligible uncertainty in bombarding energy. Natural lead targets were made from high-purity lead (<0.001% Bi). Evaporation was from a Mo filament at a distance of 18 inches from the foils. Enriched lead isotope targets were prepared, with special precautions because of the limited quantity of the lead available. Table I gives the isotopic compositions of the leads used. The spectroscopic analyses showed chemical impurities to be negligible.

The evaporation method was used to obtain the desired uniform density of lead on the targets. The distance from the point of evaporation to the aluminum foil blanks was taken to be about 3 inches. This is the minimum distance that permitted the preparation of 35 foils simultaneously, or enough for one bombardment. To obtain uniform density of deposit on the foils, a curved foil holder was designed. It was found that the required shape could be approximated closely by a hemisphere 4.5 inches in diameter suspended with the center of the hemisphere 1.25 inches above the point of evaporation. The foil blanks were clamped to the inside of the holder. The holder was perforated where foil blanks could not be fitted together. A glass container was placed outside the holder to catch the lead isotope that escaped. This lead could then be recovered by dissolving it from the glass with acid. The holder was positioned over the cone with care, since the dimensions are fairly critical. Each evaporation required 300 mg of lead isotope to obtain a density of $\sim$1 mg/cm^2 on the foils. Approximately 30% of the lead was deposited on the foils, 20% on the target holder and 50% on the glass (from which it could be recovered).

TABLE I. Isotopic abundances of the target leads.

Lead isotope	Abundance of isotope (%) Natural lead	Enriched Pb^{206}	Enriched Pb^{207}	Enriched Pb^{208}
204	1.4	0.172	0.119	<0.2
206	26.3	64.93	7.73	1.9
207	20.8	18.35	61.06	7.8
208	51.5	16.55	31.09	90.3

Evaporation of the lead took place from a small graphite cone with an included angle of 120°. This was slightly larger than the angle subtended by the entire foil holder. The cone was made of high-purity graphite and was heated white-hot in vacuum to drive off volatile impurities. The cone was heated by electron bombardment from a surrounding filament. Heat shielding protected the foils from heat radiated by the filament. The lead for the evaporation formed a small bead in the bottom of the cone. Trial evaporations were made with ordinary lead. First trials gave a dark-colored deposit. This was attributed to heating effects due to the proximity of the foils to the hot cone. In later evaporations the temperature of the cone was maintained low enough that it required about thirty minutes for the lead to evaporate. The deposit obtained was shiny and adherent. Variation in lead density on adjacent foils averaged two or three percent. Thus the foils were acceptable for bombardment. Variation in the absolute density of deposit for different regions of the holder was somewhat larger. This, however, does not affect the accuracy of the experiment.

The enriched Pb^{206} and Pb^{207} leads were supplied in the form of the monoxide. The monoxide was reduced to metallic lead by heating it in a hydrogen atmosphere. The reduction was carried out in a graphite cone. The metallic lead collected as beads. Weighings showed that the reduction was complete. The enriched Pb^{208} was supplied as the chloride. This was first converted to the oxide and then reduced.

B. Bombardment

The energy spread of the external beam of the cyclotron was reduced by allowing it to travel about 3 feet in the fringing magnetic field of the cyclotron magnet. The beam traveled in a tube connected to the cyclotron vacuum system with $\frac{1}{8}$-inch-wide collimating slits at front and back.[6,7] The tube was hinged in the middle and could be aligned on the beam by remote

[6] The apparatus is an improved version of that used by Kelly[3] and Kelly and Segrè.[7]

[7] E. L. Kelly and E. Segrè, Phys. Rev. **75**, 999 (1949).

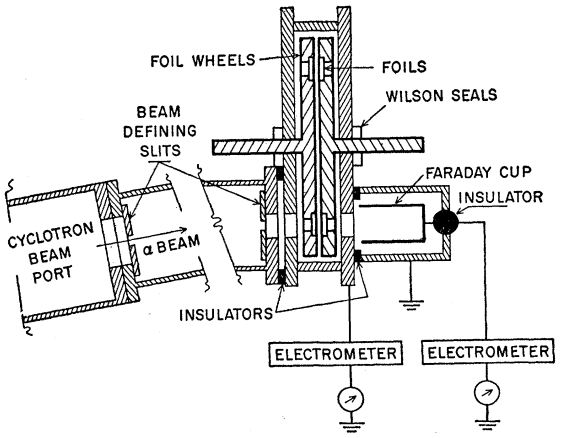

FIG. 1. Schematic diagram of the target apparatus.

control. Two foil wheels containing absorbers and the target were located on the end of the tube. A Faraday cup was placed behind the foil wheels to measure the transmitted beam. Figure 1 is a schematic diagram of the target apparatus.

The beam energy was determined from the mean range of the alpha beam in aluminum. Ranges in aluminum were converted to energy by means of the experimental range-energy relation of Bichsel and Mozley.[8–11] The target foils were bombarded in stacks with the lead film facing the beam. Ranges in the target stacks were calculated to the center of each lead film. The lead thickness was converted to aluminum equivalent with the aid of the range-energy tables of Aron, Hoffman, and Williams.[12] The stopping-power ratios obtained were compared to those experimental values for the stopping-power ratio of bismuth to aluminum which were measured by Kelly.[13] The agreement was good; moreover, the conversion is insensitive to inaccuracies of the relative stopping power, since the lead films are thin.

An effort was made to maintain constant those cyclotron parameters affecting the beam energy. The target assembly was operated by remote control so that the beam need not be turned off and on with consequent uncertainties in energy. The range of the beam was observed to drift somewhat during the cyclotron warmup period. A range curve was taken just before bombardment, the target was bombarded for about ten hours, and a range curve was taken after bombardment. The drift in range during bombardment was generally less than 1 mg/cm² Al. Range straggling of the beam was $R_{\text{extr}}-R_0/R_0=1.2\%$, where R_{extr} is the extrapolated range and R_0 is the mean range. The theoretical range straggling in Al is 0.9%.[14]

The beam current was kept at about 0.1 μa. It was found that higher beam levels caused heating damage to the lead foils. The beam was integrated with University of California Radiation Laboratory feedback-type electrometers, using a 1-μf input capacitor. The capacitor was automatically discharged at a preset voltage and the output traced on a Speedomax recorder. The integrating capacitor was calibrated to 0.2% on an impedance bridge. As a further check the capacitor was compared to a Bureau of Standards 10^8-ohm resistor by alternating them in the input circuit with a constant-current input. The relative values agreed to within 0.5%. The over-all calibration of the electrometer system was checked by measuring an accurately known current. This current was generated by placing a Leeds and Northrup potentiometer voltage in series with the Bureau of Standards resistor. The output of the electrometer was found to be 1.5% low. This is a reasonable correction, since the voltage dividing network at the output consists of several 1%-tolerance resistors.

Secondary electron emission from the Faraday cup was suppressed by the strong fringing field of the cyclotron magnet. The vacuum was essentially that of the cyclotron tank, eliminating possible errors from gas ionization. The Faraday cup, foil wheel, and associated cables were checked for current leakage by using a dummy current source. The Faraday cup was also checked for leakage under actual bombardment conditions by charging it up with the beam and then isolating it by stopping the beam on the foil wheel. Checks were also made to insure that rf pickup was negligible. No appreciable drifting of the zero point of the battery-operated electrometers was observed during the bombardments.

C. Counting

Gross alpha counting was done with standard UCRL ZnS-5819 scintillation counters and scalers. The scintillation counters were calibrated by comparison to a 2π-geometry ionization chamber. The ionization chamber was 1.5 cm deep and was filled with argon at 1.7 atmos. The counting efficiency of the scintillation counters was found to be 97% of that of the ionization chamber. The counting efficiency of the ionization chamber was taken to be 50%. Corrections for self-absorption and backscattering were made by the methods of Rossi and Staub.[15] Typical corrections to observed counting rates were +3.5% to account for

[8] H. Bichsel and R. F. Mozley (private communication).
[9] H. Bichsel and R. F. Mozley, Phys. Rev. **94**, 764 (A) (1954).
[10] For a given energy, the range from Bichsel and Mozley's experiments is about 1.2% higher than the theoretical values of Smith.[11]
[11] J. H. Smith, Phys. Rev. **71**, 32 (1947).
[12] Aron, Hoffman, and Williams, U. S. Atomic Energy Commission Report AECU-663, second revision, 1949 (unpublished).
[13] E. L. Kelly, Phys. Rev. **75**, 1006 (1949).
[14] H. Bethe and J. Ashkin, *Experimental Nuclear Physics*, edited by E. Segrè (John Wiley and Sons, Inc., New York, 1953), Vol. I, p. 244.
[15] B. B. Rossi and H. H. Staub, *Ionization Chambers and Counters* (McGraw-Hill Book Company, Inc., New York, 1949), National Nuclear Energy Series, Manhattan Project Technical Section, Vol. 2, Div. V.

TABLE II. Cross sections for alpha-induced reactions on lead.

Alpha energy (Mev)	Pb^{206} $(\alpha,2n)$ (barns)	Pb^{206} $(\alpha,3n)$ (barns)	Pb^{206} $(\alpha,4n)$ (barns)	Pb^{207} (α,n) (barns)	Pb^{207} $(\alpha,3n)$ (barns)	Pb^{208} $(\alpha,2n)$ (barns)	Pb^{208} $(\alpha,4n)$ (barns)
18				0.002			
19				0.006		0.001	
20	0.002			0.025		0.0065	
21	0.010			0.067		0.036	
22	0.047			0.106		0.112	
23	0.137			0.10		0.249	
24	0.29			0.07		0.42	
25	0.48			0.03		0.56	
26	0.61				0.00	0.68	
27	0.72				0.005	0.80	
28	0.83				0.008	0.90	
29	0.93				0.014	0.97	
30	1.01				0.04	1.01	
31	1.05	0.03			0.12	0.97	
32	1.04	0.14			0.28	0.85	
33	0.94	0.33			0.51	0.66	
34	0.77	0.64			0.73	0.48	
35	0.58	0.94			0.93	0.37	
36	0.43	1.18			1.08	0.285	
37	0.31	1.38			1.20	0.225	0.02
38	0.22				1.29	0.183	0.03
39	0.18		0.00		1.35	0.155	0.05
40	0.16		0.02		1.35	0.140	0.14
41	0.15		0.08		1.30	0.128	0.28
42	0.14		0.19		1.19	0.117	0.44
43	0.11		0.35		1.05	0.109	0.63
44	0.09		0.57		0.88	0.099	0.83
45	0.08		0.81		0.72	0.090	1.01
46	0.07		1.04		0.59	0.081	1.17
47	0.08		1.22		0.49	0.074	1.25
47.5			1.27			0.070	

self-absorption and -1% for backscattering. The scintillation counters had broad plateaus and were essentially free from background. An alpha standard was counted periodically. The observed counting rate remained constant to within 1%.

The polonium isotopes 206, 208, 209, and 210 were identified and their relative abundance determined by alpha pulse-height analysis. The sample was placed in a gridded ionization chamber; the output pulses were fed into a 48-channel pulse-height analyzer.[16] The alpha counts of each isotope were thus separated according to the energy of the alpha particles. The extremely thin samples required for the pulse-height analysis were prepared by dissolving the targets in HNO_3, boiling with HCl to destroy the nitrate, and plating onto Ag blanks by electrodeposition. The chemistry of each sample was carried out in new glassware. In addition, blanks were carried through the chemistry as a precaution against cross-contamination. With care, it was found possible to plate out a desired amount of activity to within $\pm 25\%$. The amount plated out was controlled in order to control counting losses in the analyzer. Sample counting rates were adjusted so that the statistical error would be larger than the register losses in most cases. Test analyses of samples with various counting rates indicated no serious deviations from statistical errors. For the natural lead targets every other sample was analyzed. All the enriched isotope samples were analyzed.

Decay analysis was applied to the alpha activities of Po^{206} and Po^{207}. In addition, the gamma activities of these two isotopes were counted with a NaI scintillation counter. For Po^{207} the relative gamma activity was more accurately determined than the relative alpha activity, owing to the extremely small alpha-branching ratio. Therefore relative cross sections for Po^{207} were based on the gamma counting. The absolute values of the cross sections were normalized to the alpha counting.

Aluminum blanks were spaced throughout the target foil stacks. These blanks were counted to detect any activity induced in the aluminum or its impurities. The use of blanks also checked against the possibility of transfer of activity from the lead foils by recoil or from handling. No alpha activity was found on any of the blanks. The aluminum did show some gamma activity. This background activity was subtracted from the gamma activity of the lead foils.

The over-all operation of the equipment was checked by a trial bombardment of bismuth. A few points were obtained on the excitation function $Bi^{209}(\alpha,2n)At^{211}$. These agreed well with the data of Kelly and Segrè.[7]

[16] Ghiorso, Jaffey, Robinson, and Weissbourd, *The Transuranium Elements: Research Papers*, edited by Seaborg, Katz, and Manning (McGraw-Hill Book Company, Inc., New York, 1949). Paper No. 16.8, National Nuclear Energy Series, Plutonium Project Record, Vol. 14B, Div. IV.

TABLE III. Cross sections for the production of Po^{206}, Po^{208}, Po^{209}, and Po^{210} by alpha-particle bombardment of natural lead. $\sigma_j = \Sigma_i a_i \sigma_{ij}$ are listed where a_i is the fractional abundance of lead isotope i and σ_{ij} is the cross section in barns for production of polonium isotope j from lead isotope i. The σ_j are from direct measurements.

	Po^{208}			Po^{209}			Po^{210}			Po^{206}
Alpha energy (Mev)	Run I (barns)	Run II (barns)	Run III (barns)	Run I (barns)	Run II (barns)	Run III (barns)	Run I (barns)	Run II (barns)	Run III (barns)	Run III (barns)
18.3				0.001			0.0014			
19.1		0.0002			0.004			0.0058		
19.3	0.0002			0.004			0.0057			
20.3	0.0004			0.018			0.0167			
20.4		0.0006			0.02			0.020		
21.3	0.004	0.004		0.030	0.04		0.046	0.049		
22.2	0.014	0.016		0.06	0.07		0.090	0.099		
23.0	0.040			0.11			0.156			
23.1		0.045			0.11			0.168		
23.9	0.074			0.16			0.220			
24.7		0.104			0.12			0.283		
24.8	0.102			0.09			0.278			
25.5		0.137			0.14			0.345		
25.6	0.132			0.13			0.330			
26.4	0.152			0.15			0.375			
27.1		0.19			0.17			0.43		
27.2	0.20			0.21			0.44			
27.8		0.21			0.19			0.47		
28.0	0.22			0.20			0.50			
28.7	0.23			0.21			0.51			
29.2		0.24			0.22			0.52		
29.5	0.24			0.25			0.54			
30.0		0.26			0.28			0.54		
30.2	0.26			0.34			0.56			
30.7		0.27			0.33			0.54		
30.9	0.29			0.35			0.54			
31.4		0.31			0.39			0.50		
31.6	0.34			0.31			0.51			
32.1		0.34			0.43			0.44		
32.3	0.36			0.47			0.44			
32.8		0.31			0.41			0.33		
32.9	0.37			0.55			0.371			
33.4		0.36			0.49			0.318		
33.6	0.38			0.53			0.318			
34.2	0.38			0.47			0.269			
34.6		0.36			0.53			0.229		
34.8	0.36			0.53			0.219			
35.5	0.38			0.56			0.186			
35.8		0.34			0.52			0.160		
36.2	0.36			0.60			0.156			
36.8	0.36			0.56			0.133			
37.0		0.39			0.56			0.127		
37.5	0.36			0.58			0.117			
37.8			0.36			0.61			0.107	
38.1	0.37			0.57			0.102			
38.2		0.36			0.58			0.100		
38.7	0.40			0.68			0.099			
38.9			0.37			0.67			0.090	0.02
39.3		0.39			0.64			0.086		
39.9			0.41			0.65			0.078	0.05
41.0			0.45			0.58			0.070	0.08
41.9			0.50			0.44			0.065	0.17
42.9			0.56			0.50			0.062	0.33
43.9			0.63			0.31			0.057	0.50
44.8			0.62			0.26			0.055	0.70
45.8			0.72			0.21			0.053	0.89
46.7			0.72			0.26			0.045	1.11
47.7			0.75			0.25			0.049	1.21
48.6			0.76			0.30			0.046	1.30

IV. RESULTS

A. Measured Cross Sections

Tables II to IV give the cross sections calculated from the data of this experiment. The excitation functions are plotted in Figs. 2–4. The cross-section measurements for the enriched isotopes were made at intervals of approximately 1 Mev. So that the results of the various bombardments could be combined, the cross sections were interpolated graphically to integral numbers of Mev. The error introduced by the interpolation was smaller than the uncertainties of the measurements.

The estimated relative errors in the cross sections are listed in Table V. These were calculated from the counting statistics of the pulse analysis and gross counting with an additional 2% error for nonuniformity of the isotope targets. In addition to the relative errors, the error in absolute value of the cross sections is estimated to be ±3%.

TABLE IV. Cross section in barns for the reaction $Pb^{208}(\alpha,3n)Po^{209}$.

Alpha energy (Mev)	Cross section (barns)
30.3	0.0
31.0	0.3
31.6	0.7
32.9	0.4
34.1	0.8
34.7	0.8
35.9	1.1
37.1	0.9
38.2	0.9
39.3	1.0
40.3	1.1
41.4	0.8
42.4	1.0
43.4	0.7
44.4	0.5
45.3	0.8
46.2	0.6
47.1	0.5

The cross sections calculated from the enriched-isotope data were combined and compared with the natural-lead results for the production of the various Po isotopes. Good agreement was obtained in magnitude and energy dependence. The yield of Po^{210} from natural lead was about 4% higher than calculated from the $Pb^{208}(\alpha,2n)Po^{210}$ and $Pb^{207}(\alpha,n)Po^{210}$.

The energies for the lead bombardments are estimated to be correct within ±0.2 Mev, allowing for observed drifts of the cyclotron energy.

B. Yields of Po^{206}, Po^{207}, and Po^{209}

The cross sections for $Pb^{206}(\alpha,3n)Po^{207}$ and $Po^{206}(\alpha,4n)Po^{206}$ depend on the alpha branching ratios of Po^{207} and Po^{206}. The values used here are from Kelly.[3] The uncertainty of these branching ratios is larger than the errors discussed above.

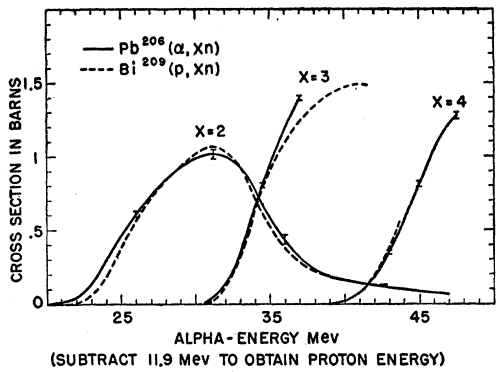

FIG. 2. Comparison of the excitation functions for $Pb^{206}(\alpha,xn)$ from this experiment and $Bi^{209}(p,xn)$ from reference 3.

The Po^{206} yields could be determined in three ways. One depended largely on the pulse analysis, the second depended largely on decay analysis. The third was from the relative yields given directly by the gamma counting. All three showed excellent agreement. The half-life of Po^{206} has been determined to be 8.8±0.1 days from decay analysis.

The decay data of Kelly[17] were reanalyzed to check the half-life of Po^{207}. The value computed was 6.2±0.1 hours, compared to 5.7 hours found by Templeton, Howland, and Perlman.[4] However, the effect on the calculated cross section was found to be negligible. The absolute normalization of the reaction $Pb^{206}(\alpha,3n)Po^{207}$ is uncertain by ±6%, owing largely to alpha counting statistics. The reaction $Pb^{206}(\alpha,3n)Po^{207}$ was not calculated above 37 Mev because of the interference from the reaction $Pb^{206}(\alpha,4n)Po^{206}$.

The half-life for Po^{209} was taken to be 100 years from the estimate of Kelly.[3] The half-life calculated from recent measurements is found to be 103 years.[18] Because of the long half-life, counting statistics were relatively poor. No attempt was made to calculate the excitation functions for $Pb^{206}(\alpha,n)Po^{209}$ and $Pb^{207}(\alpha,2n)Po^{209}$.

V. DISCUSSION

A. Test of the Predictions of Bohr's Compound Nucleus Theory

The comparison between the excitation functions for $Pb^{206}+\alpha$ and $Bi+p$ is illustrated in Fig. 2. The compound nucleus produced in both cases is Po^{210}. The proton curves have been shifted by adding 11.9 Mev to the proton energy to match the curves. In order to satisfy the prediction of Bohr's theory it must be possible to shift the curves so that

$$\sigma(p,2n):\sigma(p,3n):\sigma(p,4n)=\sigma(\alpha,2n):\sigma(\alpha,3n):\sigma(\alpha,4n).$$

Inspection of Fig. 2 reveals that this condition is well satisfied. However, the compound nucleus theory

[17] E. L. Kelly (private communication).
[18] Andre, Huizenga, Mech, Ramler, Rauh, and Rocklin, Phys. Rev. **101**, 645 (1956).

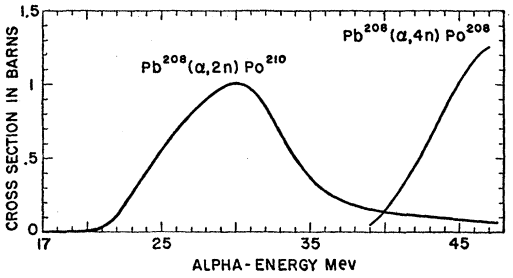

FIG. 3. Excitation functions for $Pb^{208}(\alpha,2n)Po^{210}$ and $Pb^{208}(\alpha,4n)Po^{208}$.

requires that the curves be shifted by an amount which would produce the compound nucleus with the same excitation energy. The transformation from center-of-mass coordinates to laboratory coordinates must be made in calculating the exact energy shift required. The relation between the proton and alpha energies in the laboratory system must be

$$E_p = aE_\alpha - b,$$

where $a=206/209$, $b=(210/209)\Delta Mc^2$, and $\Delta M = M_{Bi} + M_H - M_{Pb206} - M_{He}$. The value of b found by matching the experimental curves is 11.3 ± 0.4 Mev. The transformation of coordinates introduced a correction of about 0.6 Mev. The uncertainty is estimated from the uncertainties in the bombarding energies. Kelly[3] estimated the error in the proton bombardment energies for the Bi+p experiments to be ±0.3 Mev. It should be pointed out that Kelly experienced some difficulty in determining the beam energy of the linear accelerator but found good agreement between several bombardments. The alpha bombardment energies are considered to be accurate to ±0.2 Mev. An internal check was also made between all the lead bombardments. Since the targets were not completely separated isotopes, some reactions were visible in all targets. The excitation functions for these reactions could be compared to test the energy determinations. The reactions $Pb^{206}(\alpha,4n)Po^{206}$ and $Pb^{208}(\alpha,2n)Po^{210}$ were especially useful for this purpose. The intercomparisons supported the above estimate of the error in bombardment energy.

We note that the comparison between the lead and bismuth cross sections is independent of the uncertainty in the alpha branching ratios of Po^{206} and Po^{207} since the same values were used in both calculations. For the comparison the proton ranges were converted to energy by using the Bichsel and Mozley[8] range-energy table.

We now calculate b from the masses. We note that ΔM contains the difference between the Bi^{209} and Pb^{206} masses. This difference may be taken from the table of Stern[19] or the more recent table of Glass, Thompson, and Seaborg.[20] The mass difference needed here is the same in both tables. The mass tables in the region of lead are based on decay energies and neutron binding energies. For example, we may link Bi^{209} and Pb^{206} as follows:

$$Pb^{206} \xrightarrow[6.73\ \text{Mev}]{+n^0} Pb^{207} \xrightarrow[7.38\ \text{Mev}]{+n^0} Pb^{208} \xrightarrow[3.87\ \text{Mev}]{+n^0}$$

B.E. B.E. B.E.

$$Pb^{209} \xrightarrow[0.64\ \text{Mev}]{\beta^-} Bi^{209}.$$

The data are taken from Glass, Thompson, and Seaborg. All of the energies listed are measured energies. The difference in mass values is estimated to be accurate to ±0.1[20] or ±0.2 Mev.[19] The value of b calculated from the mass values is 10.5 ± 0.2 Mev.

The calculated value of b, 10.5 ± 0.2 Mev, is to be compared to the experimental value of 11.3 ± 0.4 Mev. The experimental value thus appears to be higher than the calculated value by 0.8 ± 0.5 Mev, or by an amount just outside of the probable error. Because of this possible disagreement with theory the Ghoshal[2] experiment has been re-examined. Ghoshal compared the excitation functions for $Cu^{63}+p$ and $Ni^{60}+\alpha$. In the laboratory system the energies are again related by

$$E_p = aE_\alpha - b,$$

where $a=60/63$, $b=(64/63)\Delta Mc^2$, and $\Delta M = M_{Cu63} + M_H - M_{Ni60} - M_{He}$. We note that the proton curves are stretched by 1.3 Mev more at the highest energies relative to the lowest energies. The value of b found from matching the experimental curves is 6.4 ± 1.0 Mev. The uncertainty is taken from Ghoshal's estimate. For comparison the value of b may be calculated from the mass values. The Cu^{63} and Ni^{60} masses have recently been measured with high precision by Quisenberry.[21] The result for b is 3.83 ± 0.02 Mev. The difference between the observed and calculated b is 2.6 ± 1 Mev. This difference is also considered to be outside of the estimated errors. In both the Cu—Ni and Bi—Pb comparisons the observed b is larger than the b calculated from the masses. The discrepancy is greater for the Cu—Ni comparison.

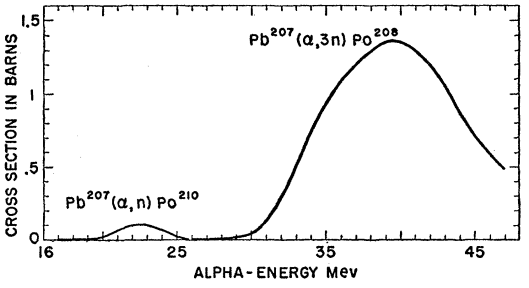

FIG. 4. Excitation functions for $Pb^{207}(\alpha,n)Po^{210}$ and $Pb^{207}(\alpha,3n)Po^{208}$.

[19] M. O. Stern, Revs. Modern Phys. **21**, 316 (1949).
[20] Glass, Thompson, and Seaborg, J. Inorg. Nuc. Chem., **1**, No. 1, 3 (1955).
[21] A. O. C. Nier (private communication).

TABLE V. Estimated relative errors in the cross sections.

Reaction	Energy (Mev)	Error (barns)	Percent error
$Pb^{206}(\alpha,2n)Po^{208}$	21	0.002	15
	22	0.002	5
	26	0.02	3
	31	0.03	3
	35	0.03	5
	38	0.02	9
	42	0.02	13
	46	0.02	24
$Pb^{206}(\alpha,3n)Po^{207}$	32	0.006	4
	35	0.02	2
	37	0.03	2
	39	0.04	2
$Pb^{206}(\alpha,4n)Po^{206}$	40	0.007	100
	43	0.01	3
	45	0.02	2
	47	0.03	2
$Pb^{207}(\alpha,n)Po^{210}$	20	0.0007	3
	22	0.004	4
	23	0.006	6
	24	0.008	11
	25	0.01	33
$Pb^{207}(\alpha,3n)Po^{208}$	27	0.009	180
	31	0.01	10
	34	0.02	3
	36	0.03	3
	40	0.04	3
	44	0.04	4
	46	0.04	6
$Pb^{208}(\alpha,2n)Po^{210}$	20	0.0002	3
	22	0.002	2
	25	0.01	2
	30	0.02	2
	35	0.01	3
	40	0.004	3
	45	0.005	5
$Pb^{208}(\alpha,4n)Po^{208}$	38	0.01	40
	40	0.01	7
	42	0.02	4
	44	0.03	3
	46	0.03	3

Barring an unknown systematic error in the experiments, the discrepancy between the observed and calculated energy shift b could indicate a small deviation from Bohr's theory. It may be possible to explain the deviation in terms of the presence of some direct interactions resulting in the ejection of neutrons. The energy spectrum of such neutrons would in general be different from that of evaporated neutrons. Furthermore, since both the bombarding particles and the target nuclei are different the importance of direct interactions could be different in the two cases being compared. We have not made any calculations to test these ideas.

B. General Features of the Excitation Functions in the Region of Lead

The alpha bombarding energies ranged from about 20 Mev to 47 Mev. In this energy region the number of neutrons observed to be emitted in reactions on lead increases from one to four as the energy increases. A slight indication of the beginning of the reaction $Pb^{207}(\alpha,5n)Po^{206}$ was seen at 47.5 Mev. The excitation functions exhibit a characteristic competition between the reactions involving the emission of various numbers of neutrons. The excitation functions for reactions on the various lead isotopes are very similar. They are also similar to the excitation functions for alpha and proton bombardment of bismuth.

In Fig. 5 all of the available excitation functions for lead and bismuth have been graphed for comparison. The energy scale is that for $Pb^{206}+\alpha$. The energy scales for the other excitation functions have been shifted to give a visual match of apparent thresholds. The observed shifts and the shifts calculated from mass values available in the tables of Stern[19] and Glass, Thompson, and Seaborg[20] are listed in Table VI.

The $(a,2n)$, $(a,3n)$, and $(a,4n)$ reactions are remarkably similar for all target nuclei. The (a,n) reactions do not match in shape as well as the others. The reaction $Pb^{208}(\alpha,n)Po^{211}$ is probably not as accurate as the other (a,n) reactions since it was necessary to sum the cross sections for the formation of the two very short-lived Po^{211} isomers. The observed similarity of the excitation functions is in general agreement with the expectations of the statistical theory. We note, for example, that the evaporation theory predicts that the excitation functions for $(a,2n)$ reactions on neighboring nuclei will be nearly the same if their thresholds are matched.

The energy shifts which were employed to match the curves in Fig. 5 may be compared to the differences in thresholds. The reaction $Pb^{207}(\alpha,n)Po^{210}$ was compared to the reaction $Bi^{209}(p,n)Po^{209}$. The relative energy shift observed to match thresholds is $E_p-E_\alpha=-11.9$ Mev. The shift calculated from the difference between the thresholds is -9.7 Mev. The discrepancy is 1.6 Mev, including the correction to center-of-mass coordinates. The discussion of errors in Sec. V,A also applies in general to this section. The errors for the (α,n) curves are somewhat higher.

The observed energy shift for $Pb^{208}(\alpha,2n)Po^{210}$

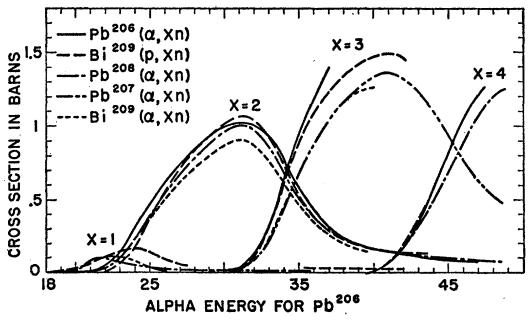

Fig. 5. Comparisons of the excitation functions for lead and bismuth. The curves for lead are based on the data of this experiment. The $Pb^{208}(\alpha,n)$ data are taken from reference 5, the bismuth data from references 3 and 7. The energy scale applies to reactions on Pb^{206}. For the energy scales of the other curves see Table VI.

TABLE VI. Energy shifts for Fig. 5. The bombarding energy was increased by the amount given under "observed energy shift."

Reaction	Observed energy shift (Mev)	Shift calculated from masses (Mev)
$Pb^{206}(\alpha,xn)Po$	≡0	≡0
$Pb^{207}(\alpha,n)Po^{210}$	0[a]	...
$Pb^{207}(\alpha,3n)Po^{208}$	1.3	...
$Pb^{208}(\alpha,n)Po^{211}$	0.2[a]	...
$Pb^{208}(\alpha,2n)Po^{210}$	1.1	0.1
$Pb^{208}(\alpha,4n)Po^{208}$	1.7	...
$Bi^{209}(p,xn)Po$	11.9[b]	10.4
$Bi^{209}(\alpha,2n)At^{211}$	0.8	−0.6
$Bi^{209}(\alpha,3n)At^{210}$	1.3	...

[a] Matched to $Bi^{209}(p,n)Po^{209}$.
[b] See Sec. V, A, for discussion including correction to center-of-mass coordinates.

relative to $Pb^{206}(\alpha,2n)Po^{208}$ is $E_\alpha(Pb^{208})-E_\alpha(Pb^{206})=-1.1$ Mev. The calculated shift is −0.1 Mev. The correction from laboratory to center-of-mass coordinates is negligible here. The observed shift was verified in the enriched Pb^{206} bombardment where both reactions were present, giving a check independent of the beam energy determination. The discrepancy is outside of the errors.

The observed energy shift for $Bi^{209}(\alpha,2n)At^{211}$ relative to $Pb^{206}(\alpha,2n)Po^{208}$ is $E_\alpha(Bi^{209})-E_\alpha(Pb^{206})=-0.8$ Mev. The calculated shift is +0.6 Mev. The discrepancy is 1.4 Mev. The observed energy shift for $Bi^{209}(\alpha,3n)At^{210}$ relative to $Pb^{207}(\alpha,3n)Po^{208}$ is $E_\alpha(Bi^{209})-E_\alpha(Pb^{207})=0.0$ Mev. The calculated shift is −1.6 Mev.

Thus the observed energy shifts disagree with the shifts calculated from the differences in thresholds by one or two Mev. We note that the measured excitation functions are being compared well above their thresholds. The cross sections are not as reliable near the threshold because of interference between reactions and straggling effects.

From the comparison of the reactions $Pb^{208}(\alpha,4n)Po^{208}$ and $Pb^{206}(\alpha,4n)Po^{206}$, the Po^{206} mass is calculated to be 206.0446±~0.002 amu. From the comparison of the reactions $Pb^{207}(\alpha,3n)Po^{208}$ and $Pb^{206}(\alpha,3n)Po^{207}$, the Po^{207} mass is calculated to be 207.0452±~0.002 amu. These masses are calculated on the Stern scale. On the Glass, Thompson, and Seaborg scale they would be 206.0443 and 207.0449. The errors are estimated from the discrepancies between the observed and calculated energy shifts for the reactions involving known masses.

Deuteron-induced reactions should be considered separately. Kelly[3] and Kelly and Segrè[7] have measured the excitation functions for the reactions (d,n), (d,p), $(d,2n)$, and $(d,3n)$ on Bi. When the deuteron-induced reactions are compared to the alpha- and proton-induced reactions on Bi, qualitative differences are seen. The differences are most pronounced for the (d,n) and (d,p) reactions. This is probably because of the importance of stripping processes.[22] The $(d,2n)$ excitation function is more similar to the $(\alpha,2n)$ and $(p,2n)$ excitation functions, indicating that compound nucleus formation is probably more important.

[22] D. C. Peaslee, Phys. Rev. 74, 1001 (1948).

C. Total Cross Sections

In Fig. 6 total cross sections have been plotted as a function of the alpha energy in the center-of-mass system. The cross sections for Pb^{206} neglect the contribution from $Pb^{206}(\alpha,n)Po^{209}$. Therefore the Pb^{206} data is plotted only above 27 Mev where the cross section for $Pb^{206}(\alpha,n)Po^{209}$ is expected to be less than ~0.02 b. The slight rise of the Pb^{206} cross sections above the dotted line between 35 and 40 Mev may be due to an error in the alpha branching ratio of Po^{207} used here. The total cross sections for Pb^{207} are plotted only below 21 Mev where the contribution from $Pb^{207}(\alpha,2n)Po^{209}$ should be small. The Pb^{208} cross sections include the $Pb^{208}(\alpha,n)Po^{211}$ reaction from reference 5. The two Pb^{208} points at high energies are somewhat lower than the dotted line but the uncertainties are large due to the poor statistics for the $Pb^{208}(\alpha,3n)Po^{209}$ reaction.

For comparison the theoretical total cross sections calculated by Weisskopf[23] and by Blatt and Weisskopf[24] are shown. Values for lead were obtained by graphical interpolation. In general the experimental points fit the Weisskopf calculations with $r_0=1.5\times10^{-13}$ cm. The Blatt and Weisskopf values for $r_0=1.5\times10^{-13}$ cm are about 25% lower than the experimental points for energies above 25 Mev. This is well outside the experimental errors. The radius of interaction used by Blatt and Weisskopf is $R=r_0A^{\frac{1}{3}}+\rho$, $\rho=1.2\times10^{-13}$ cm. The radius used in the Weisskopf calculations is not stated. The quoted barriers for $r_0=1.5\times10^{-13}$ cm are slightly lower in the Weisskopf table, but the main difference with the Blatt and Weisskopf table comes from the large difference in the quoted cross sections for a given ratio of alpha energy to barrier height.

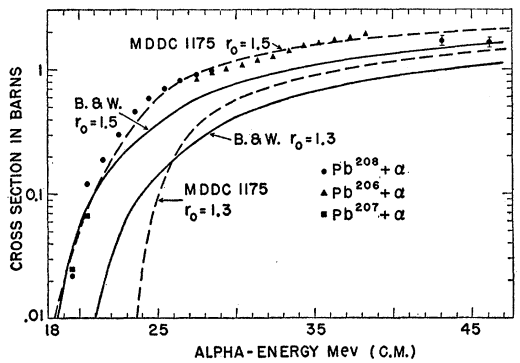

FIG. 6. Total cross sections for alphas on lead. Experimental points are shown. Theoretical values are shown in dotted lines (reference 23) and solid lines (reference 24).

[23] V. F. Weisskopf, *Lecture Series in Nuclear Physics*, U. S. Atomic Energy Commission Report MDDC-1175 (U. S. Government Printing Office, Washington, D. C., 1947).
[24] J. M. Blatt and V. F. Weisskopf, *Theoretical Nuclear Physics* (John Wiley and Sons, Inc., New York, 1952).

ACKNOWLEDGMENTS

The author is grateful to Professor Emilio Segrè for suggesting this experiment and supporting its execution. The author thanks Dr. Elmer Kelly for instructive discussion concerning his bismuth experiments.

Mr. Albert Ghiorso lent the use of the alpha pulse-height analyzer. Mr. Dan O'Connell of the Accelerator Technicians, University of California Radiation Laboratory, carried out the enriched-lead isotope evaporations. The enriched Pb^{206} and Pb^{207} were supplied by the Oak Ridge National Laboratory, the Pb^{208} by the nuclear chemistry group of the Radiation Laboratory. The high-purity natural lead and its spectroscopic analysis were supplied by Mr. George M. Gordon, U.C. Division of Mineral Technology. Dr. Hans Bichsel and Dr. R. F. Mozley kindly supplied their range-energy data for protons in aluminum. Dr. Ann Birge lent the use of some target apparatus. The 60-inch cyclotron staff gave efficient cooperation for the bombardments. Mr. George Merkel assisted with the bombardments.

PHYSICAL REVIEW VOLUME 103, NUMBER 3 AUGUST 1, 1956

Excited States in B^{10}†

JERRY B. MARION*
Kellogg Radiation Laboratory, California Institute of Technology, Pasadena, California
(Received April 23, 1956)

Energy levels in B^{10} have been investigated by observing the neutrons from the $Be^9(p,n)B^9$ reaction and the γ rays from the $Be^9(p,\alpha\gamma)Li^6$ reaction in the range of bombarding energy from 2 Mev to 5 Mev. At $E_p=2.562\pm0.006$ Mev both the neutrons and the γ rays are resonant. The width of the γ-ray peak is 38 ± 3 kev while the width of the neutron peak is 85 ± 10 kev. The results are analyzed in terms of two B^{10} states at 8.89 Mev which probably are the analogs to the 7.37- and 7.54-Mev states in Be^{10}. The neutron reduced widths for the B^{10} states are in good agreement with those for the Be^{10} states (which is to be expected on the basis of charge symmetry of nuclear forces) if the neutron and γ-ray resonances have $J=3^+$, $T=1$ and $J=2^+$, $T=1$, respectively. In addition, a broad resonance in the neutron yield at $\theta=90°$ near 3.2 Mev indicates a wide level ($\Gamma\approx0.7$ Mev) in B^{10} at 9.5 Mev. Angular distributions of the neutrons have been measured and total cross sections obtained at bombarding energies of 2.56, 2.92, 3.06, 3.56, and 4.56 Mev.

INTRODUCTION

THE proton bombardment of Be^9 at energies above 2 Mev has revealed several resonances in the yield of neutrons from the $Be^9(p,n)B^9$ reaction and of γ rays from the $Be^9(p,\alpha\gamma)Li^6$ reaction. Neutron resonances have been found at 2.56 Mev,[1–4] 4.70 Mev,[3,4] and 4.94 Mev[4]; a γ-ray resonance has been observed at 2.565 Mev.[3,5–7] The width of the γ-ray resonance has been determined to be 39 ± 2 kev[5–7]; however, the 2.56-Mev neutron resonance is superposed on a rising background and, although it appears to be somewhat wider than the γ-ray resonance, an accurate determination of the width has not previously been made. It is the purpose of this investigation to obtain more information concerning the 2.56-Mev resonance and to study the nature of the rising background observed in the $Be^9(p,n)B^9$ reaction.

Gamma radiation from Be^9+p can arise either from proton capture (which is relatively weak) or from the $Be^9(p,\alpha)Li^{6*}(\gamma)Li^6$ reaction involving the 3.57-Mev level in Li^6. For bombarding energies below about 5 Mev no other reactions are expected to yield γ rays. The Li^6 state at 3.57 Mev[8] has $J=0^+$, $T=1$; therefore only B^{10} states with parity $\pi=(-)^J$ and isotopic spin[9] $T=1$ can give rise to this α-particle group and the corresponding γ ray. There are no isotopic spin restrictions on the $Be^9(p,n)B^9$ reaction; consequently, neutrons can be emitted from B^{10} states which have either $T=0$ or $T=1$ while γ rays can arise only from $T=1$ states.

The 8.89-Mev state in B^{10}, corresponding to the 2.56-Mev γ-ray resonance probably has[10] $J=2^+$, $T=1$. The $T=1$ character of this state has been confirmed by Malm and Inglis[6] and by Marion, Weber, and Davis[11]

† A portion of this work was done at the Rice Institute, Houston, Texas, and was supported in part by the U. S. Atomic Energy Commission; at the California Institute of Technology, the work was supported by the joint program of the Office of Naval Research and the U. S. Atomic Energy Commission.

* National Science Foundation Postdoctoral Fellow.

[1] W. J. Hushley, Phys. Rev. **67**, 34 (1945).

[2] Richards, Smith, and Browne, Phys. Rev. **80**, 524 (1950).

[3] Hahn, Snyder, Willard, Bair, Klema, Kington, and Green, Phys. Rev. **85**, 934 (1952).

[4] Marion, Bonner, and Cook, Phys. Rev. **100**, 91 (1955).

[5] R. B. Day and R. L. Walker, Phys. Rev. **85**, 582 (1952).

[6] R. Malm and D. R. Inglis, Phys. Rev. **95**, 993 (1954).

[7] Kington, Cohn, Bair, and Willard, Oak Ridge National Laboratory Semiannual Progress Report, ORNL-1975, September, 1955 (unpublished).

[8] F. Ajzenberg and T. Lauritsen, Revs. Modern Phys. **27**, 77 (1955).

[9] The isotopic spin restriction is, of course, much less stringent because of the possibility of large isotopic spin impurities.

[10] R. J. Mackin, Jr., Phys. Rev. **94**, 648 (1954).

[11] Marion, Weber, and Davis (to be published).